Materials Advances

ROYAL SOCIETY OF CHEMISTRY

PAPER

View Article Online
View Journal | View Issue

Cite this: *Mater. Adv.*, 2025, 6, 365

Self-assembling PEGylated mannolipids for liposomal drug encapsulation of natural products†

Leila Mousavifar,‡[a] Mukul R. Gupta,‡[a] Madleen Rivat,[a] Aly El Riz,[a] Abdelkrim Azzouz,[a] Jordan D. Lewicky,[b] Alexandrine L. Martel,[b] Hoang-Thanh Le[bcd] and René Roy*[a]

The chemical synthesis of modified neoglycolipids is reported in an effort to further improve the drug delivery properties of previously described mannosylated liposomes possessing alkyl linkers in the aglyconic moiety. A self-contingent strategy that overcomes previous synthetic limitations was used to produce neoglycolipids that have a single exposed α-D-mannopyranoside residue, an aromatic scaffold, and two lipid tails with varied alkyl chains. The lipid tails were built from 3,5-dihydoxybenzoic acid possessing two alkyl chains of twelve to sixteen carbons (C_{12}–C_{16}). The azido-ending carbohydrate precursor, harboring a hydrophilic triethylene glycol, was prepared by glycosidation of mannose pentaacetate with triethylene glycol monotosylate using standard Lewis acid-catalysed conditions. The carboxylic acid-ending lipid tails were directly ligated to the azido mannopyranoside residue using a modified Staudinger chemistry. The formation of stable spherical vesicles of controllable sizes (≈100 nm) was confirmed by dynamic light scattering (DLS), TEM, and AFM experiments. The values of critical micelle concentration (CMC) of mannnolipids were also determined by DLS using variations of scattered light as a function of concentrations. The CMC values obtained from the C_{12} to the C_{16} alkyl chains were 1.76×10^{-6}, 3.87×10^{-6}, and 3.86×10^{-6} mol L^{-1}, respectively. The bio-relevance of the mannosylated glycolipids were also demonstrated using their cross-linking abilities with the leguminous lectin Concanavalin A from *Canavalia ensiformis* which is a homotetrameric mannose-binding protein. In addition, the glycolipids were biocompatible, enhanced cell uptake of lipophilic cargos, and improved the human plasma stability of entrapped quercetin.

Received 7th October 2024,
Accepted 1st December 2024

DOI: 10.1039/d4ma01007h

rsc.li/materials-advances

1. Introduction

Nanocarrier-based therapeutics for the treatment of cancer and infectious diseases constitute an appealing approach as both passive and active vaccines or drug delivery system.[1–4] Passive directing of nanoparticles (NPs) is usually controlled by altering the size, charges, shapes, and surface properties of the carriers, while active targeting is usually achieved by incorporating selected cell surface ligands for specific receptor-mediated uptake. Several examples using mannoside-coated nanomaterials of varied compositions have made striking progress due to the exceptional physicochemical properties of these mannosylated NPs.[5–7] The targeting of therapeutic agents and vaccines to antigen presenting cells (APCs)[8,9] and the blood brain barrier (BBB)[10,11] have proven useful in both cases, respectively.

Amongst NPs, mannosylated liposomal preparations[12–14] are particularly attractive since they combine the above requirements combined to active cell-specific targeting to mannose-receptors (MRs).[5–9,15,16] Due to their amphiphilic nature, nano-sized liposomes that mimic the phospholipid membrane of cells allows encapsulation of both hydrophilic and hydrophobic drugs or vaccine components. Moreover, they also showed high selectivity towards the MRs which can be further improved by the proper choices of linkers, the number and architectures of the mannopyranoside moieties.[17] This can be achieved by manipulating both the transcytosis capacity and variable degrees of expression of mannose receptors expressed at the cell surface. MRs are ubiquitous transmembrane proteins that have been usually targeted to increase the affinity and selectivity of therapeutic-loaded NPs by altering

[a] *Glycosciences and Nanomaterial Laboratory, Université du Québec à Montréal, P.O. Box 8888, Succ. Centre-Ville, Montréal, Québec, H3C 3P8, Canada. E-mail: roy.rene@uqam.ca*
[b] *Health Sciences North Research Institute, 56 Walford Road, Sudbury, ON, P3E 2H2, Canada*
[c] *Medicinal Sciences Division, NOSM University, 935 Ramsey Lake Road, Sudbury, ON P3E 2C6, Canada*
[d] *School of Natural Sciences, Laurentian University, 935 Ramsey Lake Road, Sudbury, ON P3E 2C6, Canada*

† Electronic supplementary information (ESI) available: NMR and CMC tables and figures. See DOI: https://doi.org/10.1039/d4ma01007h

‡ These authors contributed equally.

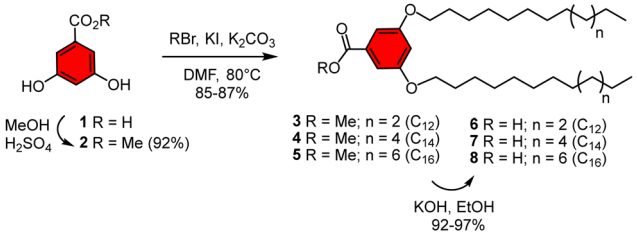

Scheme 1 Syntheses of the aromatic-bearing lipid tails **7–8** based on 3,5-dihydroxybenzoic acid (**1**).

their intrinsic architectures, including the use of mannose mimetics.[18]

In our previous work, a straightforward chemical strategy has been developed towards carbohydrate-based neoglycolipids.[19] Their preparation relied on the use of a sugar bearing alkyne functionality in the aglyconic portion. Sequential photocatalyzed thiol–yne ligation led, when required, to either homo- or hetero-functionalized lipid tails.[19] One of the drawbacks of this chemistry was that it generated a new stereocenter and related glycolipids were isolated as inseparable mixtures of diastereomers. Ultimately, this is not an ideal situation in terms of pharmacological development, where defined and exact stereochemistry is required. In addition, the synthetic strategy led to neoglycolipids having short linkers between the sugar headgroups and the lipid tails, which might impact the ultimate availability of the sugar residues for interaction with their cognate carbohydrate binding receptors. Even though liposomes previously generated from the self-assembly of neoglycolipids originating from mannosylated alkyne-containing aglycones have been shown to be particularly useful toward the stabilization of entrapped peptides, they still necessitated stabilization of the lipid bilayers as delivery system.[20–22]

In an effort toward additional improvements of these earlier mannosylated-forming liposomes, the chemical syntheses of a series of neoglycolipids having an exposed sugar residue, an aromatic scaffold lacking stereocenters, and two lipid tails with *varied alkyl chains* forming liposomal nanocarriers of controllable sizes was described.[23] In the actual strategy, a hydrophilic *triethylene glycol linker* was selected because of its better hydrophilic/hydrophobic balance, while anticipated to possess better bioavailability profiles once released from their lipid counterparts. The sugar-linked lipid architectures consisted of a 3,5-dihydoxybenzoic acid framework having two alkyl chains of twelve to sixteen carbons. The azido-ending carbohydrates and the carboxylic acid-ending lipid architecture were ligated using a Staudinger chemistry to generate neoglycolipid structures that were chemically stable.

2. Results and discussions

2.1 Neoglycolipid synthesis and characterization

In continuation of our efforts to further improve the stability and physicochemical properties of our liposomal delivery system, it was anticipated that increasing the hydrophilic balance of the water-soluble head group, in replacement of the hexyl linker, would provide improved access to the MRs' binding sites. For this, the syntheses of the neoglycolipids were performed using a two stages convergent approach as described in Schemes 1 and 2, which involved the preparation of the lipid tails (Scheme 1) and a α-D-mannopyranoside head group (Scheme 2). First, the synthesis of the lipid architectures was based on a 3,5-dihydroxybenzoic acid scaffold (**1**) as before. Protection of the acid functionality as a methyl ester (MeOH, H_2SO_4) afforded known methyl ester **2**[23] in 92% yield, which

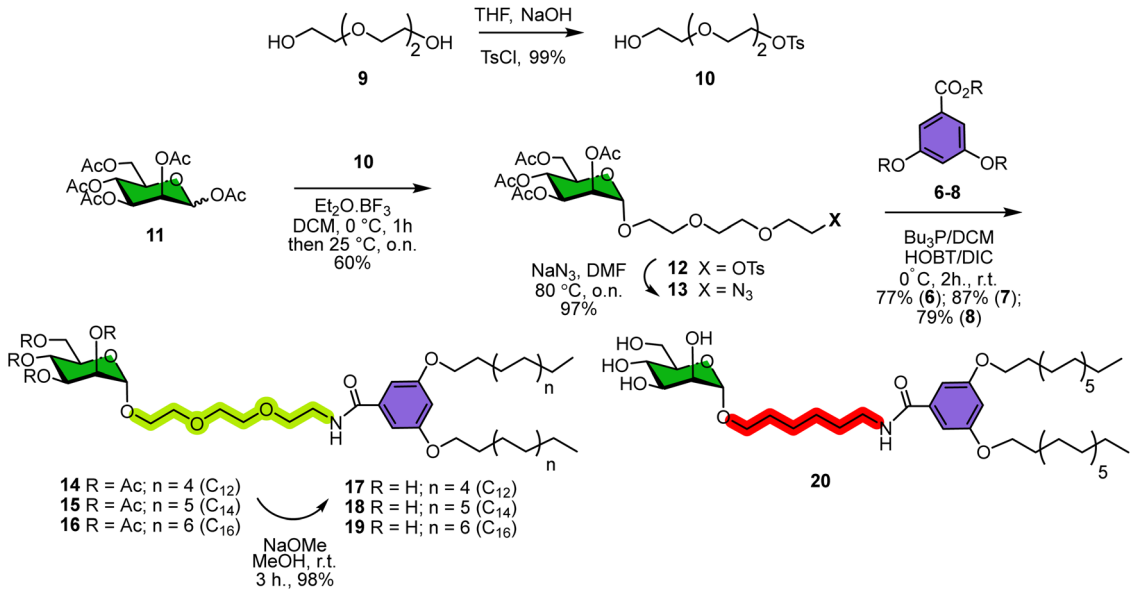

Scheme 2 Syntheses of mannosylated neoglycolipids (**17–19**) using a one-pot modified Staudinger reaction between azide **13** and acids **6–8** with a triethylene glycol linker at the sugar residue. Previous compound **20**, prepared with a hexyl linker, was also prepared for comparison.[23]

was alkylated with C_{12}–C_{16} alkyl bromides (RBr, KI, K_2CO_3, DMF, 80 °C) to provide intermediates **3–5** in 86–87% yields. Methyl esters hydrolysis (KOH, EtOH) provided lipid tails **6–8** in 92–97% yields (Scheme 1). The procedure was analogous to the one previously published for related glycodendrimersomes.[24–26]

A triethylene glycol linker was initially chosen to provide the final mannolipids with a more hydrophilic head group when compared to previous versions.[27,28] The necessary α-D-mannopyranoside moiety was prepared from mannose pentaacetate **11**, which was initially glycosidated with 2-[2-(2-tosylethoxy)-ethoxy]ethanol (**10**) using BF_3-OEt_2 in DCM as Lewis acid catalyst to give tosylate **12** in 60% yield.[29] Substitution of the tosylate by an azide functionality was accomplished using standard conditions (NaN_3, NaI, DMF, 80 °C) to afford previously described azide **13** in 97% yield prepared using a slightly different route.[30] The direct chemical ligation between the above lipid moieties **6–8**, bearing an acid functionality, and the azide **13** were done by a Staudinger reaction (Bu_3P, HOBt, DIC, DCM). This choice was dictated in order to avoid typical *O*- to *N*-acyl shift usually observed as by-products when peracetylated sugars are present with free amines. This approach gave rise to peracetylated neoglycolipids **14–16** in good yields (77–87%). The procedure appears to be more practical to the one using glycosylation of the lipids tails harboring alcohol head groups because of better controls in the anomeric stereoselectivity.[27,28] Uneventful *trans*-esterification under Zemplén conditions (NaOMe, MeOH) provided unprotected mannosylated liposome precursors **17–19** in almost quantitative yields. Final neoglycolipids were fully characterized by ^{1}H- and ^{13}C-NMR spectroscopy and by mass spectrometry (see ESI†).

We evaluated the beneficial choice of the more hydrophilic triethylene glycol linker in **17–19** over the previous *n*-hexyl aglycone in **20**. For this, we calculated the topological surface area tPSA and *C* log *P* of the glycosidic portions of **18**, once released from the lipid tail groups, which was shown to be 143.86 and −2.56 while they were 125.4 and −0.97 for **20**. Hence, **18** should present a better pharmacological profile.

Interestingly, we were able to crystalize methyl ester **4** in dichloromethane: methanol containing a C_{14} lipid chain and the m.p. was recorded at 69.4–70.2 °C. In the crystal, the molecules are planar, and the lateral C_{14} lipid chains adopt a fully extended zig-zag conformation with a bending angle approximately of 160° between the two chain ends. Not surprisingly, the two alkyl chains spread laterally to the benzene ring which formed a torsion angle between C_{23}–O_1–C_4–C_3 of −176.8° (details to be published separately). The structure is analogous to a previous crystal containing two C_{12} alkyl chains.[31] This conformation is obviously not *a priori* compatible with their self-assembly, nevertheless, these precursors readily formed stable mannosylated liposomes and work is in progress to further deepen these behaviors.

2.2 Liposome characterization by DLS, TEM, and AFM

The simplest method for the self-assembly of amphiphilic molecules into vesicles and liposomes involves the injection of their solution in a water-miscible solvent, such as ethanol or THF, into water or buffers.[32] This methodology has been shown to be efficient for the self-assembly of previously described amphiphilic analog prepared by our unprecedented thiol–yne ligation between sugar alkynes and thiols[19] and from the hexyl-linked mannolipids.[20–23] The injection method was also found suitable using stable amphiphilic Janus dendrimers into monodisperse vesicles called glycodendrimersomes, as previously described.[24–26] The resulting self-assemblies were first analyzed by dynamic light scattering (DLS) for size and polydispersity (PDI). Table 1 shows the size and DPI of compounds **17–19** which varied from 98.4 (**18**) to 147.0 (**19**) nm when pre-dissolved in EtOH followed by injection into doubly distilled water. These measurements indicated that the mannolipids formed small unilamellar vesicles (SUV). The critical micelle (CMC) concentrations were evaluated by DLS using the intensity of the scattered light (k_{cps}) from a series of solutions ranging from 0.40×10^{-6} to 5.7×10^{-4}. The CMC values for mannolipids **17–19** were 1.76×10^{-6}, 3.87×10^{-6}, and 3.86×10^{-6} mol L^{-1}, respectively (see ESI†).

Table 1 Average diameter (DLS) and polydispersity indexes (PDI) of mannosylated liposomes using the injection method. Solutions of the neoglycolipids (5 mg mL^{-1} in ethanol) were injected (100 μL) into 1.9 mL of doubly distilled water to provide final volumes of 2 mL, as these conditions were found optimal toward the targeted liposomal diameter

Compounds	Lipid tail size	Diameter (nm)	PDI
17	C_{12}	119.6 ± 0.53	0.19
18	C_{14}	98.4 ± 0.47	0.16
19	C_{16}	147.0 ± 0.45	0.13

Because compound **18** (C_{14}) was produced in good yield and was easier to purify, as well as showing the best overall behaviour and appropriate size for our next applications, we also evaluated the effect of its concentration on the SUV formation. Table 2 illustrate that the size of the liposomes varied from 64.8 to 119.1 nm. We next turned to evaluate the time stability of liposomes formed from **18**. Importantly and as seen from Table 2, the sizes of the SUV were stable after 2 months. In contrast, mannolipid **20**, harboring a hexyl-linked mannoside was readily precipitating soon after their self-assembly into larger initial aggregates (766 nm). Thus, this unbalanced hydrophilic/hydrophobic combination was found unsuitable for the following experiments and further confirmed

Table 2 Effect of concentration of compound **18** (C_{14}) on the size and stability of liposomes formation by the injection method from stock solutions (5 mg mL^{-1} in ethanol) followed by injection of 100 μL into 1.9 mL of doubly distilled water (total volume 2 mL)

Concentration (mg mL^{-1})	**18** (0 days)		**18** (30 days)		**18** (60 days)	
	D_h (nm)	PDI	D_h (nm)	PDI	D_h (nm)	PDI
0.75	64.8 ± 1	0.14	63 ± 1	0.14	154 ± 6	0.48
1.25	63.8 ± 1	0.18	63 ± 1	0.17	273 ± 11	0.40
2.50	76.7 ± 0.9	0.11	74 ± 1	0.16	196 ± 2	0.33
5.0	98.4 ± 1	0.16	89 ± 1	0.15	ND	ND
10.0	119.1 ± 2	0.17	116 ± 2	0.17	128 ± 2	0.17

Conserved at 4 °C prior to size determination. ND: not determined.

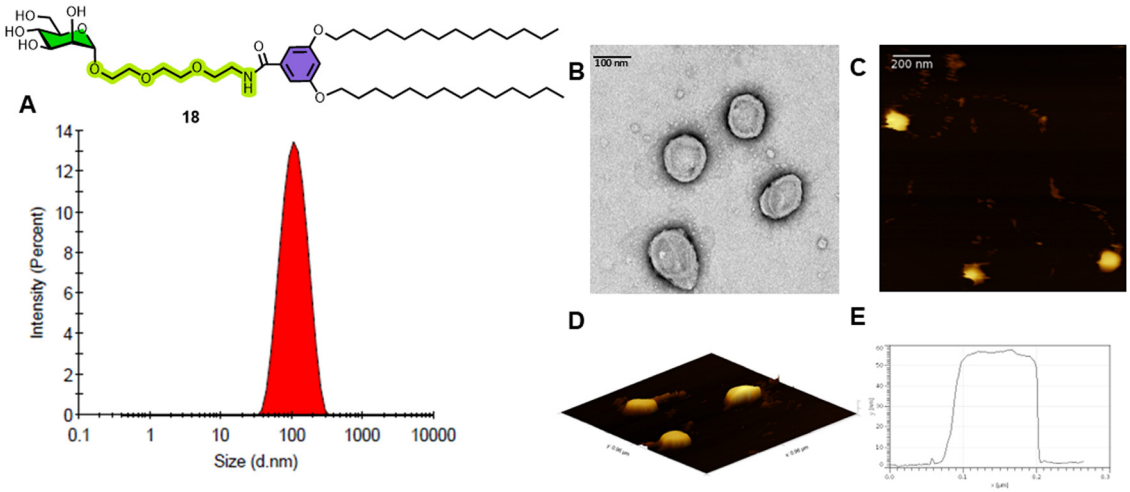

Fig. 1 Compound **18** at 5.0 mg mL^{-1} in EtOH injected into water to a final concentration of 400 nM. (A) DLS size distribution pattern (D_h 98.4 ± 1, PDI 0.16); (B) TEM image of the resulting liposomes in water (scale bar at 100 nm); (C) and (D) AFM images of **18** as dried vesicles (scale bar at 200 nm); (E) AFM height profile on mica measured at ambient humidity.

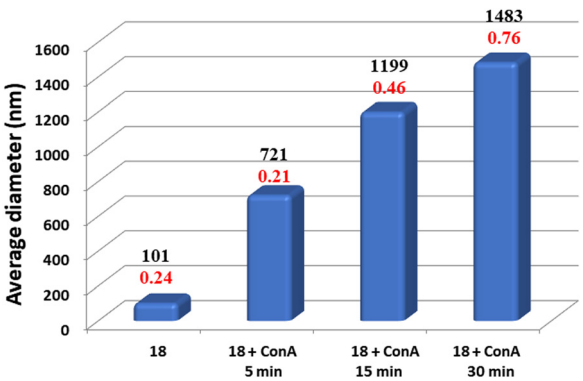

Fig. 2 DLS measurements of mannosylated liposomes **18** (C_{14}) (0.1 mL of a 10 mg mL^{-1} ethanol solution) in the presence of Concanavalin A (ConA) (2 mL) of a 0.15 mg mL^{-1} in PBS buffer. Polydispersity indexes (PDI) are indicated in red.

our choice for a more hydrophilic triethylene glycol linker. Fig. 1 further illustrates the typical liposomal DLS pattern (1A) observed from **18**, the TEM results (1B), together with the three-dimensional AFM pictures (1C–E). We concluded that **18** presented a better balance between the hydrophilic and hydrophobic balances to impart desired size, longer term stability, and adequate CMC values typical with natural glycolipids.

2.3 Interactions of mannosylated liposomes with concanavalin A

The bio-relevance of the carbohydrates displayed at the periphery of the vesicles to interact with protein receptors was qualitatively evaluated by agglutination experiments (cross-linking) using DLS measurements in the presence of concanavalin A (ConA), a mannose-binding leguminous lectin systematically used as role model.[33–37] This C-type lectin occurs as a homotetramer of 26.4 kDa per subunit with a molecular weight of 104–112 kDa and a diameter of ∼8 nm. The cross-linking abilities of the liposomes formed from compound **18** in the presence of ConA as a function of time is illustrated in Fig. 2. The rapid formation of larger aggregates from 101 nm (**18** alone) and the steady increase after 30 min (1483 nm) in the presence of ConA clearly demonstrated the accessibility of the α-D-mannopyranoside residues to the four carbohydrate binding sites of ConA and the resulting cross-linking aggregation (Table 3). With a

Table 3 Size variations of the mannosylated liposome **18** (0.1 mL of a 10 mg mL^{-1} ethanol solution) in the presence and absence of the leguminous lectin ConA (2 mL of a 0.15 mg mL^{-1} PBS buffer solution), together with selective cross-linking inhibition of aggregate formations with methyl α-D-mannopyranoside (0.1 mL of a 50 mg mL^{-1} in water). Methyl α-D-galactopyranoside (0.1 mL of a 50 mg mL^{-1} in water) showed no size decrease in the presence of ConA

Concentration of **18** (mg mL^{-1})/time (min)	Cpd **18**		Cpd **18** + ConA		Cpd **18** + ConA + Me α-D-Man		Cpd **18** + ConA + Me α-D-Gal	
	D_h[a] (nm)	PDI	D_h (nm)	PDI	D_h (nm)	PDI	D_h (nm)	PDI
10	101 ± 0	0.24						
10/17			3.668 ± 3	0.34				
10/20							3.109 ± 8	1.0
10/25					835 ± 1	0.58		
10/30					643 ± 2	0.57		
10/35					639 ± 2	0.51		
10/45					162 ± 1	0.19		

[a] Size distribution was recorded by intensity.

diameter of only ~8 nm, the full coverage of the mannoliposomes (~101 nm) by the lectin (~8 nm) could not account for the large diameters observed for the cross-linked lattices (up to 1483 nm). To illustrate the sugar selectivity of the aggregation process, methyl α-D-mannopyranoside was added after the formation of the cross-linked aggregates. After 20 min. of inhibition, the DLS showed a steady return to a smaller non-aggregated size of 162 nm. In contrast, using methyl α-D-galactopyranoside, a ligand not recognized by the ConA lectin, the large size of the aggregate remained unchanged.

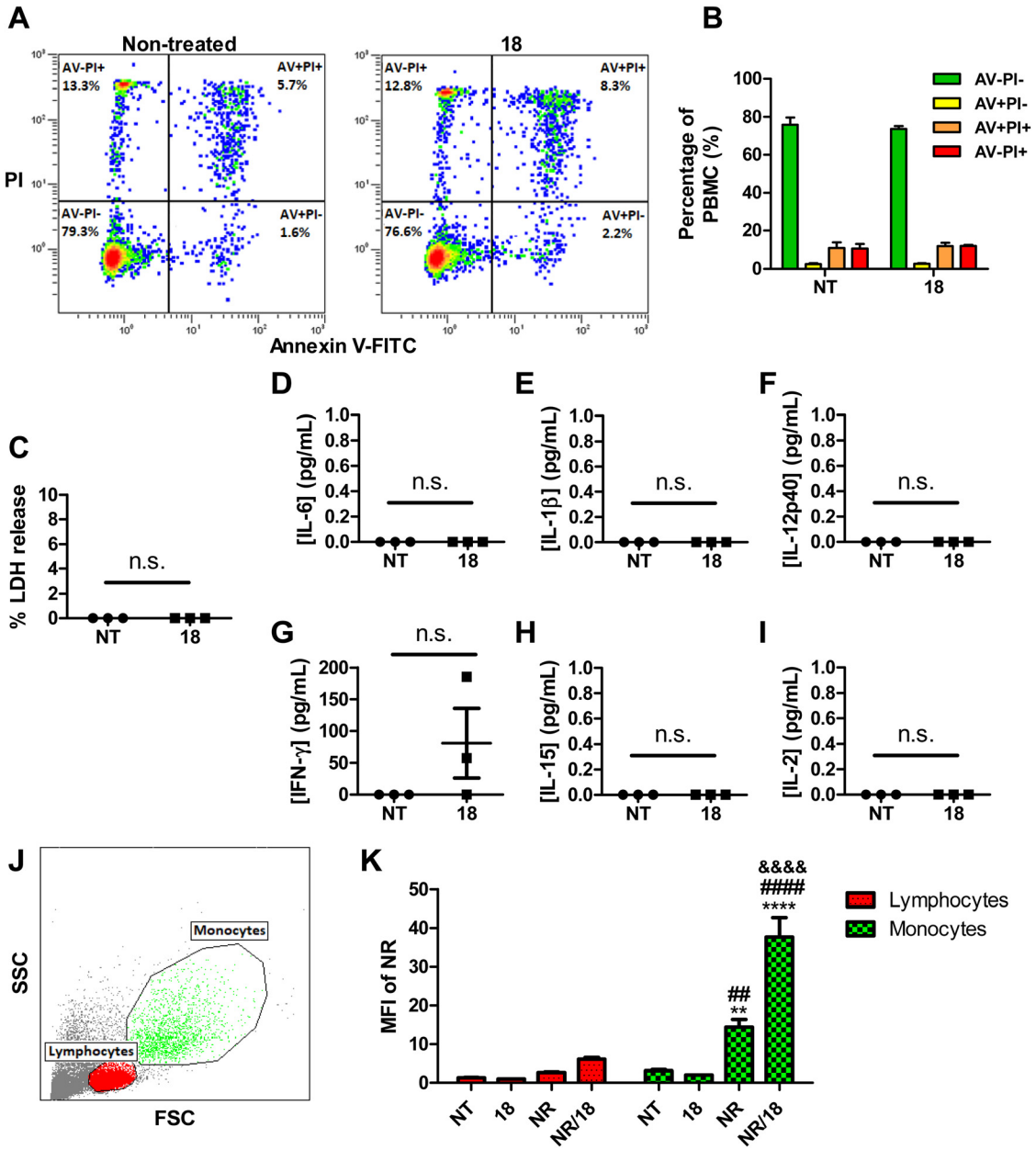

Fig. 3 Liposomes obtained from compound 18 are non-toxic and enhance uptake in PBMC. (A) and (B) Apoptosis and necrosis were assessed by flow cytometry using Annexin V (AV) and propidium iodide (PI) staining following a 48 hours incubation with 50 μg mL^{-1} of **18** where: (A) shows a representative dot plots for one donor and (B) shows the summary of the data where no data were identified as being significant as compared to a non-treated (NT) control. (C) LDH release was measured after 48 hours of treatment with 50 μg mL^{-1} of **18**. Supernatant levels of (D) IL-6, (E) IL-1β, (F) IL-12p40 were measured after 48 hours, and (G) IFN-γ, (H) IL-15, (I) IL-2 were measured after 7 days of treatment with 10 μg mL^{-1} of **18**. (J) and (K) Nile red (NR) uptake in PBMC was measured by flow cytometry after 1 hour of treatment with 1 μg mL^{-1} of NR alone or encapsulated in 10 μg mL^{-1} of 18. J. shows the gating strategy using the forward (FSC) and side (SSC) scatter and (K) shows the uptake (MFI: mean fluorescence intensity) where $^{**}p < 0.01$ and $^{****}p < 0.0001$ as compared to the lymphocytes for the respective treatment, $^{\#\#\#}p < 0.001$ and $^{\#\#\#\#}p < 0.0001$ as compared to non-treated for the respective cell population, and $^{\&\&\&\&}p < 0.0001$ as compared to NR alone for the respective cell population. All statistical analysis were performed as a two-way ANOVA with Bonferroni *post hoc* test (B) and (K) or as an unpaired *t*-test (C)–(I). All data represented as the mean ± SEM of 3 different PBMC donors. n.s.: not significant.

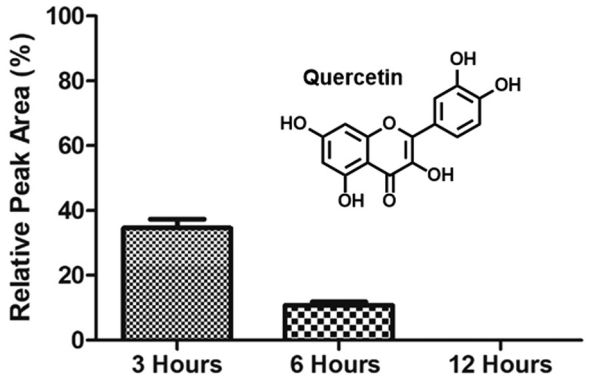

Fig. 4 Plasma stability of quercetin. Quercetin was combined with human plasma and incubated at 37 °C. The levels of quercetin remaining at various time points were analyzed by RP-HPLC in the presence of 0.1% trifluoroacetic acid and detected by absorbance at 254 nm. Quercetin amounts were calculated relative to the quantities determined at time point zero, and data are shown as the average ± SEM of three separate experiments.

These results clearly suggest that the SUVs formed from the new neoglycolipid monomer are selective for the mannoside residues and that they remained stable even in the presence of a multimeric protein receptor.

2.4 Biocompatibility and cell uptake studies in peripheral blood mononuclear cells (PBMC)

The safety profile of **18** was investigated in PBMCs isolated from three healthy volunteers. Using an Annexin V/propidium iodide assay and a lactate dehydrogenase assay respectively, we established that **18** does not induce apoptosis/necrosis, nor does it disturb membrane integrity (Fig. 3a–c). Compounds **18** also does not induce the secretion of pro-inflammatory cytokines making it non-immunogenic (Fig. 3d–i). When entrapping a lipophilic drug cargo (Nile Red) within **18**, we observed a large significant increase in drug uptake in monocytes, and a small non-significant increase in lymphocytes (Fig. 3j and k). This is unsurprising as antigen-presenting cells are known to have high expression of mannose receptors.[8,9]

2.5 *In vitro* evaluation of the protective plasma stability of quercetin

Quercetin is an important member of the plant flavonoids best known for its anti-inflammatory, antihypertensive, and having vasodilator effects.[38] The oral bioavailability of quercetin in humans is very low. One investigation estimated it to be less than 1%.[39] Intravenous injection of quercetin showed fast decay in concentration with a half-life of 2.4 hours.[39] Quercetin undergoes rapid and extensive metabolism by glucuronidation, therefore the biological effects presumed from *in vitro* studies would be unlikely to apply *in vivo*.[40]

Quercetin stability in human plasma was assessed *via* RP-HPLC using a modified version of our previously reported methods.[23] The results indicate that quercetin is rapidly degraded in plasma, with complete degradation occurring between 6–12 hours (Fig. 4).

The ability of the manno-liposomal delivery system to protect quercetin and prevent its degradation in human plasma was assessed *via* RP-HPLC using a modified version of our previously reported methods.[23,41–43] The delivery systems (DS) consisted of the **18** in combination with cholesterol, which was previously shown to provide improved the physicochemical properties of the resulting liposomal particles. Firstly, we established that approximately 80% of quercetin at a 1 : 5 weight ratio was entrapped within the DS, showing good entrapment efficacy (Fig. 5a). The results also indicated that the delivery

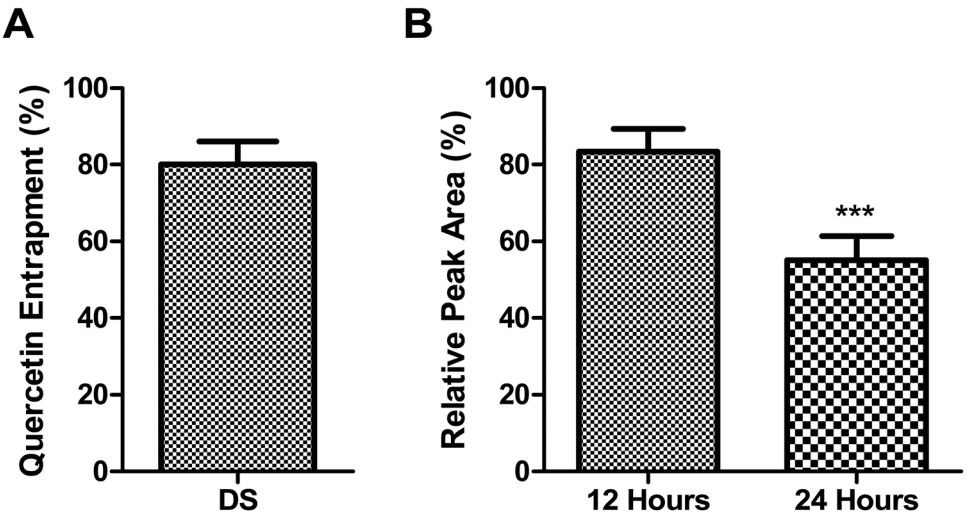

Fig. 5 Entrapment (A) and plasma stability (B) of mannoliposome-entrapped quercetin. Quercetin was combined with a glycoliposomal delivery systems (DS) assembled from **18** and cholesterol at a 1 : 5 ratio of quercetin : DS (w/w). (A) Entrapment was assessed by measuring free levels of quercetin in the supernatant and comparing it to samples devoid of DS. (B) For plasma stability, particles were incubated in human plasma at 37 °C, with the levels of quercetin remaining at various time points analyzed and calculated relative to quercetin quantities at time point zero. Quercetin levels were analyzed by RP-HPLC in the presence of 0.1% trifluoroacetic acid and detected by absorbance at 254 nm. Data are shown as the average ± SEM of three separate experiments. ***$p < 0.001$ as compared to respective 12 hours time point.

system greatly extend the stability of quercetin in plasma beyond 24 hours (Fig. 5b).

3. Conclusions

This work successfully reports the chemical syntheses of a new series of neoglycolipids harboring exposed α-D-mannopyranoside residue linked to a triethylene glycol spacer. This hydrophilic linker led to mannosylated liposomes with improved long-term stability when compared to the analogous hexyl linker previously used as drug delivery system. The sugar moiety, having a terminal azide functionality, was directly ligated through a modified Staudinger reaction to lipids tails of C_{12} to C_{16} attached to a 3,5-disubstituted benzoic acid scaffold. Even though the lipid precursor of the C_{14} lipid chains adopts a full extended zig-zag conformation when crystalized, with a bending angle approximately of 160° between the two chain ends, the resulting sugar-bound neoglycolipids could still form stable SUV of about 100 nm as demonstrated by DLS, TEM, and AFM. As opposed to related glycodendrimersomes having two sugar head groups and four lipidic alkyl chains of various length, the size of the SUVs formed by the injection methods remained constant with varied initial ethanolic concentrations of the liposome precursors. Moreover, the SUVs formed by the C_{14} alkyl chains were stable for at least two months when stored at 4 °C. The SUVs were also able to bind in a multivalent fashion to the homotetrameric leguminous lectin Concanavalin A as seen from size-dependent DLS experiments. The newly formed mannosylated SUVs were also used as drug delivery systems in a preliminary experiment by encapsulating the highly plasma unstable plant flavonoid quercetin (half-life of 2.4 hours) known to possess anti-oxidant, anti-inflammatory, and anti-cancer properties. Overall, the mannosylated liposomes assembled with a hydrophilic aglycone, two alkyl chains (C_{14} lipid chain length), mounted on an aromatic scaffold, showed promising properties as delivery system for natural products as well as for brain delivery and cancer immunotherapy.[41,42] The fully synthetic neo-mannolipids described herein offers several advantages over more conventional phospholipids in terms of ease of synthesis, scalability, long-term stability of the resulting vesicles, together with better control of hydrophilic/hydrophobic balances which confer adjustable liposomal size distributions.

4. Materials and methods

4.1 Instruments

All reactions in organic medium were performed in standard oven dried glassware under an inert atmosphere of nitrogen using freshly distilled solvents stored over molecular sieves. Solvents were deoxygenated, when necessary, by bubbling nitrogen through the solution. All reagents were used as supplied without prior purification and obtained from Sigma-Aldrich Chemical Co. (Toronto, ON, Canada). Reactions were monitored by analytical thin-layer chromatography (TLC) using silica gel 60 F254 precoated plates (E. Merck, Darmstadt, Germany) and compounds were visualized by 254 nm light and/or by dipping into a mixture of sulfuric acid and methanol in water or into a mixture of $KMnO_4$ and K_2CO_3 in water followed by gentle warming with a heat-gun. Purifications were performed by flash column chromatography using silica gel from Canadian Life Science (60 Å, 40–63 μm) (Peterborough, ON, Canada) with the indicated eluent. ^{1}H NMR and ^{13}C NMR spectra were recorded at 300 and/or 600 MHz, 75 and/or 150 MHz, respectively, on a Bruker spectrometer (300 MHz and 600 MHz) (Milton, ON, Canada) and Varian spectrometer (600 MHz) (Milton, ON, Canada). All NMR spectra were measured at 25 °C in the indicated deuterated solvents. Proton and carbon chemical shifts (d) are reported in ppm and coupling constants (J) are reported in Hertz (Hz). The resonance multiplicities in the ^{1}H NMR spectra are described as ''s'' (singlet), ''d'' (doublet), ''t'' (triplet), and ''m'' (multiplet) and broad resonances are indicated by ''broad''. Residual protic solvent of $CDCl_3$ (^{1}H, 7.27 ppm; ^{13}C, 77.0 ppm (central resonance of the triplet)), D_2O (^{1}H, 4.80 ppm and 30.9 ppm for CH_3 of acetone for ^{13}C spectra) were used as standard. Two-dimensional homonuclear correlation ^{1}H–^{1}H COSY and ^{1}H–^{13}C HSQC experiments were used to confirm NMR peak assignments. Letters are used to NMR assignment (see ESI,† for details). High-resolution mass spectra (HRMS) were measured with a LC-MS-TOF (Liquid Chromatography Mass Spectrometry Time of Flight) (Agilent Technologies) in positive electrospray mode by the analytical platform of UQAM. Either protonated molecular ions $[M + nH]^{n+}$ or adducts $[M + nX]^{n+}$ (X = Na, K, NH_4) were used for empirical formula confirmation.

4.2 Dynamic light scattering (DLS), transmission electron microscopy (TEM), atomic force miscroscopy (AFM)

Dynamic light scattering (DLS) was performed with a Zetasizer NanoZS Malvern Instruments equipped with a 4 mW 633 nm He–Ne laser and avalanche photodiode positioned at 175° to the beam and temperature-controlled cuvette holder. Instrument parameters were determined automatically along with measurement times. Experiments were performed in triplicate.

The self-assembly of the neoglycoliposomes into vesicles and liposomes involved the injection method of their ethanolic solution into water or buffer as previously described.[22] This methodology has been shown to be efficient for the self-assembly of previously described amphiphilic mannosylated neoglycolipids into monodisperse vesicles.[30] The resulting assemblies were first analyzed by dynamic light scattering (DLS) for size, polydispersity (PDI), and stability in time. For liposome size determination, solutions of the neoglycolipids (3.5 mg) in EtOH (1.1 mL) were then diluted in distilled water (2.2 mL) to provide final concentrations of 1.06 mg mL^{-1} as these conditions were found optimal toward the targeted liposomal diameter.

4.2.1 Critical micelle concentration (CMC). CMCs were determined using a Malvern Zetasizer Ultra (MAL1301351) (Malvern Instruments Limited, UK) equipped with a 4 mW He–Ne laser operating at a wavelength of 633 nm. Scattered light was detected at an angle of 173°, an optical arrangement known as non-invasive back scatter (NIBS) optic arrangement that maximizes the detection of scattered light while maintaining

Table 4 Solvent gradient program for the analysis of quercetin plasma stability and glycoliposomal entrapment using water (A) and 20% acetonitrile in water (B), both with 0.1% trifluoroacetic acid (v/v)

	Solvent	
Time (min)	A (%)	B (%)
0	80	20
1	80	20
8	0	100
13	0	100
18	80	20
25	80	20

signal quality. Measurements were carried out in a (DTS0012) polystyrene latex cell at 25 °C. A series of solutions ranging from 5×10^{-4} to 0.044×10^{-5} mol L^{-1} was prepared from an aqueous stock solution prepared at initial concentration of 1 mg mL^{-1} of compound **17–19** in ethanol followed by 2-fold dilution in distilled water. Data processing was carried out with a computer attached to the instrument. The measurements were repeated three times in order to check their reproducibility. The CMC values for mannolipids **17–19** were 1.76×10^{-6}, 3.87×10^{-6}, and 3.86×10^{-6} mol L^{-1}, respectively. For details see ESI.†

4.2.2 Inhibition of aggregation of compound 18 with ConA in the presence of methyl α-D-mannopyranoside (Me-Man) and methyl α-D-galactopyranoside (Me-Gal) (Table 4). DLS measurements of mannosylated liposomes formed from compound **18** as above, alone and in the presence of ConA were allowed to settle for 10 min after which time DLS measurements were taken again.

Transmission electron microscopy (TEM) was acquired with Tecani-TEM (FEI, USA) instrument. Negative-staining transmission electron microscopy was performed as follow: a total of 10 μL of the suspension of liposomes formed from compound **18** (5 mg mL^{-1}, 100 μL THF + 900 μL nanopure water) was placed on a carbon-over-Pioloform as done previously.[19]

Atomic force miscroscopy (AFM) was performed on a Multimode Atomic Force Microscope NanoScope V (Digital Instruments) using OTESPA-R3 silicon probes (Bruker, France; tip radius = 7 nm, nominal spring constant = 26 N m^{-1}). For the sample preparation, a diluted dispersion of liposomes, prepared by thin-film in THF ($C_{diluted}$ = 0.5 mg mL^{-1}), was drop casted on freshly peeled Mica and dried at ambient conditions at 25 °C and ≈25–30% relative humidity. Images were recorded in air under ambient conditions as topological scans in tapping mode and analyzed using the Gwyddion 2.36 image software.

4.3 Chemical synthesis

4.3.1 Methyl 3,5-dihydroxybenzoate (2). To a solution of 3,5-dihydroxybenzoic acid (**1**) (5.00 g, 32.4 mmol, 1 equiv.) in dry methanol (40 mL, 30.5 equiv.) was added conc. H_2SO_4 (0.25 mL, 0.15 equiv.). The reaction mixture was heated at 70 °C for 7 h. The solution was evaporated under reduced pressure. The solid was treated carefully with a $NaHCO_3$ solution and the product was extracted with EtOAc. The organic phase was washed with water and brine and finally evaporated to afford **2** (5.05 g, 30.059 mmol, 92%) as a white solid whose physical characteristics are in complete agreement with the published data.[34] ^{1}H NMR (300 MHz, ($(CD_3)_2SO$)): δ (ppm) 9.66 (s, 2H, OH), 6.85 (d, 2H, $J_{ortho-para}$ = 2.2 Hz, H_{ortho}), 6.48 (t, 1H, $J_{para-ortho}$ = 2.2 Hz, H_{para}), 3.83 (s, 3H, OCH_3); ^{13}C NMR (Bruker 75 MHz, (DMSO-d_6)): δ (ppm) 166.4 (C_{Ester}), 158.7 (C_{Arom}), 131.5 (C_{Arom}), 107.3 (x2, C_{Arom}), 52.1 (COMe).

4.3.2 General procedure for methyl 3,5-bis(alkyloxy)-benzoates (3–5). Method A. The syntheses of this series of compounds followed our previously published protocols.[30] To a mixture of methyl 3,5-dihydroxybenzoate (**2**) (1.00 g, 5.95 mmol, 1 equiv.), K_2CO_3 (2.7 equiv.) and KI (0.07 equiv.) in DMF (25 mL) was added the corresponding 1-bromoalkanes (2.4 equiv.). The reaction mixture was stirred at 90 °C for 24 h. It was cooled and diluted with CH_2Cl_2 (100 mL). The solution was washed with water (2 × 15 mL) and brine (15 mL) and the organic layer was dried over anhydrous Na_2SO_4. The solvent was removed and a solid residue was obtained. The solid was filtered and washed with methanol and dried. The crude products were further purified by passing through a column of silica gel (hexanes, 1–4% EtOAc in hexanes as eluents) yielding (**3–5**) as white solids.

4.3.3 Methyl 3,5-bis(dodecyloxy)benzoate (3). White solid (2.57 g, 5.091 mmol, 86%). ^{1}H NMR (300 MHz, $CDCl_3$): δ (ppm) 7.15 (d, J = 3 Hz, 2H, H1), 6.63 (t, J = 3 Hz, 1H, H2), 3.96 (t, J = 6 Hz, 4H, H3), 3.89 (s, 3H, OCH_3), 1.77 (tt, J = 9 Hz, J = 6 Hz, 4H, H4), 1.45–1.27 (m, 36H, H5), 0.88 (t, J = 6 Hz, 6H, H6); ^{13}C NMR (75 MHz. $CDCl_3$): δ (ppm) 167.1 (C_{Ester}), 160.3 (C_{Ar}), 132.0 (C_{Ar}), 107.8 (C_{Ar}), 106.7 (C_{Ar}), 68.5, 52.3, 32.1, 29.8 (x2), 29.7 (x2), 29.5, 29.3, 26.2, 22.8, 14.3 (CH_3).

4.3.4 Methyl 3,5-bis(tetradecyloxy)benzoate (4). White solid (2.9 g, 5.170 mmol, 87%). We were able to crystalize methyl ester **4** in dichloromethane: methanol giving **4** as needles melting point at 69.4–70.2 °C. These crystals were used for X-ray crystallography. ^{1}H NMR (300 MHz. $CDCl_3$): δ (ppm) 7.16 (d, J = 3 Hz, 2H, H1), 6.63 (t, J = 3 Hz, 1H, H2), 3.96 (t, J = 6 Hz, 4H, H3), 3.89 (s, 3H, OCH_3), 1.77 (tt, J = 9 Hz, J = 6 Hz, 4H, H4), 1.44–1.26 (m, 44H, H5), 0.88 (t, J = 6 Hz, 6H, H6); ^{13}C NMR (75 MHz. $CDCl_3$): δ (ppm) 167.1 (C_{Ester}), 160.3 (C_{Ar}), 131.9 (C_{Ar}), 107.7 (C_{Ar}), 106.7 (C_{Ar}), 68.4, 52.3, 32.1, 29.8 (x3), 29.7, 29;5, 29.3, 26.2, 22.8, 14.3 (CH_3).

4.3.5 Methyl 3,5-bis(hexadecyloxy)benzoate (5). White solid (3.20 g, 5.186 mmol, 87%). ^{1}H NMR (300 MHz, $CDCl_3$): δ (ppm) 7.15 (d, J = 3 Hz, 2H, H1), 6.63 (t, J = 3 Hz, 1H, H2), 3.96 (t, J = 6 Hz, 4H, H3), 3.90 (s, 3H, OCH_3), 1.77 (tt, J = 9 Hz, J = 6 Hz, 4H, H4), 1.45–1.26 (m, 52H, H5), 0.88 (t, J = 6 Hz, 6H, H6); ^{13}C NMR (75 MHz, $CDCl_3$) δ (ppm) 167.1 (C_{Ester}), 160.3 (C_{Ar}), 131.9 (C_{Ar}), 107.8 (C_{Ar}), 106.7 (C_{Ar}), 68.4, 52.3, 32.1, 29.9, 29.8 (x2), 29.7, 29.5, 29.3, 26.2, 22.8, 14.3 (CH_3).

4.3.6 General procedure for hydrolysis of methyl ester (6–8)-method B. The syntheses of this series of compounds followed our previously published protocols.[30] A solution of methyl 3,5-bis(alkyloxy)benzoate (**3–5**) (1.00 g), 2.55 mmol, 1 equiv. with KOH (595 mg, 10.6 mmol, 4.2 equiv.) in water (7 mL) and ethanol (40 mL) were refluxed for 4 h. Then, reaction mixture was cooled to room temperature and concentrated hydrochloric acid was added carefully until pH = 1.

CH_2Cl_2 and water were added and the combined organic fractions were separated, dried over $MgSO_4$ and evaporated to yield 3,5-bis(alkyloxy)benzoic acid (**6–8**).

4.3.7 3,5-Bis(dodecyloxy)benzoic acid (6). White solid (0.775 g, 1.579 mmol, 97%). ^{1}H NMR (300 MHz, $CDCl_3$) δ (ppm) 7.22: (d, J = 3 Hz, 2H, H1), 6.69 (t, J = 3 Hz, 1H, H2), 3.98 (t, J = 6 Hz, 4H, H3), 1.79 (tt, J = 9 Hz, J = 6 Hz, 4H, H4), 1.46–1.27 (m, 36H, H5), 0.88 (t, J = 6 Hz, 6H, H6); ^{13}C NMR (75 MHz, $CDCl_3$): δ (ppm) 172.4 (CCO_2H), 160.4 (C_{Ar}), 131.1 (C_{Ar}), 108.3 (C_{Ar}), 107.6 (C_{Ar}), 68.5, 32.1, 29.8 (x3), 29.7, 29.5, 29.3, 26.2, 22.9, 14.3 (CH_3).

4.3.8 3,5-Bis(tetradecyloxy)benzoic acid (7). White solid (0.840 g, 1.536 mmol, 95%). ^{1}H NMR (300 MHz, $CDCl_3$): δ (ppm) 7.22 (d, J = 3 Hz, 2H, H1), 6.69 (t, J = 3 Hz, 1H, H2), 3.98 (t, J = 6 Hz, 4H, H3), 1.79 (tt, J = 9 Hz, J = 6 Hz, 4H, H4), 1.46–1.26 (m, 44H, H5), 0.88 (t, J = 6 Hz, 6H, H6); ^{13}C NMR (75 MHz, $CDCl_3$): δ (ppm) 172.4 (CCO_2H), 160.4 (C_{Ar}), 131.1 (C_{Ar}), 108.3 (C_{Ar}), 107.6 (C_{Ar}), 68.5, 32.1, 29.8 (x2), 29.7, 29.5, 29.3, 26.2, 22.9, 14.3 (CH_3).

4.3.9 3,5-Bis(hexadecyloxy)benzoic acid (8). White solid (1.43 g, 2.371 mmol, 97%). ^{1}H NMR (300 MHz, $CDCl_3$): δ (ppm) 7.22 (d, J = 3 Hz, 2H, H1), 6.68 (t, J = 3 Hz, 1H, H2), 3.98 (t, J = 6 Hz, 4H, H3), 1.78 (tt, J = 9 Hz, J = 6 Hz, 4H, H4), 1.45–1.26 (m, 52H, H5), 0.88 (t, J = 6 Hz, 6H, H6); ^{13}C NMR (75 MHz, $CDCl_3$): δ (ppm) 172.4 (CCO_2H), 160.4 (C_{Ar}), 131.1 (C_{Ar}), 108.3 (C_{Ar}), 107.6 (C_{Ar}), 68.5, 32.1, 29.9 (x2), 29.8 (x2), 29.5, 29.3, 26.2, 22.9, 14.3 (CH_3).

4.3.10 Syntheses of the mannolipids with triethyleneglycol linkers (14–16). 2-[2-(2-Tosylethoxy)ethoxy]ethanol (10). To a solution of triethylene glycol (**9**) (16.24 g, 108.15 mmol, 10 equiv.) in THF (45 mL) was added 6 mL of 4 M aqueous solution of NaOH at 0 °C and the resulting reaction mixture was stirred for 1 h. Using a dropping funnel, a solution of tosyl chloride (TsCl, 2.11 g, 10.82 mmol, 1 equiv.) in THF (25 mL) was added dropwise over 30 min and the reaction mixture was stirred at 0 °C for an additional 3 h. Then the reaction mixture was poured into ice-cold water (200 mL) and extracted with DCM (3 × 200 mL), dried over Na_2SO_4 and concentrated *in vacuo*. After chromatographic purification compound **10** (3.29 g m, 10.82 mmol, 99% based on the TsCl used) was obtained as colorless oil. R_f = 0.47, (DCM/acetone: 7/3); ^{1}H NMR (300 MHz, $CDCl_3$): δ (ppm) 7.73 (d, J = 8.3 Hz, 2H), 7.29 (d, J = 8.1 Hz, 2H), 4.14–4.05 (m, 2H), 3.71–3.58 (m, 5H), 3.56–3.42 (m, 6H), 2.84 (t, 1H), 2.38 (s, 3H); ^{13}C NMR (75 MHz, $CDCl_3$): δ (ppm) 144.7, 132.5, 129.6, 127.6, 72.2, 70.3, 69.8, 69.1, 68.2, 61.2, 21.2. The spectroscopic data agreed well with those of the literature.[37]

4.3.11 General procedure for the carbohydrate synthesis-method C. 2-[2-(2-Tosylethoxy)ethoxy]ethoxyl 2,3,4,6-tetra-*O*-acetyl-α-D-mannopyranoside (12). To a solution of mannose pentaacetate **11** (1 g, 2.56 mmol, 1 equiv.) in dry DCM (2.5 mL), containing dried molecular sieve, was added tosylate **10** (1.8 g, 5.98 mmol, 2.3 equiv.) at room temperature and under a nitrogen atmosphere. The solution was stirred for 1.5 h to which was added $BF_3{\cdot}OEt_2$ (2.5 equiv.) dropwise at 0 °C. The resulting mixture was stirred at room temperature for a further 24 h. The reaction mixture was washed with aq. saturated $NaHCO_3$ and the organic phase was dried over sodium sulfate, filtered and concentrated *in vaccuo*. Purification by silica gel column chromatography afforded intermediate **12** (0.96 g, 1.51 mmol, 60%) as a colorless oil: R_f = 0.35 (EtOAc/hexane, 1 : 4); ^{1}H NMR (300 MHz, $CDCl_3$): δ (ppm) 7.77 (d, J = 8.3 Hz, 2H), 7.32 (d, J = 8.0 Hz, 2H), 5.34–5.22 (m, 3H), 4.84 (d, J = 1.6 Hz, 1H), 4.25 (dd, J = 12.4, 5.2 Hz 1H), 4.17–4.08 (m, 2H), 4.09–4.05 (m, 1H), 4.05–3.98 (m, 11H), 2.12 (s, 3H), 2.12 (s, 3H), 2.07 (s, 3H), 2.01 (s, 3H), 1.96 (s, 3H); ^{13}C NMR (75 MHz, $CDCl_3$): δ (ppm) 170.6, 169.9, 169.7, 169.8, 144.7, 133.1 129.8, 127.9, 97.6, 70.7, 70.6, 70.0, 69.72, 69.5, 69.3, 69.0, 68.7, 68.4, 67.3, 66.1, 62.3, 21.6, 20.8, 20.7, 20.6, 20.5. Spectroscopic data agreed with those of the literature.[38,39]

4.3.12 2-[2-(2-Azidoethoxy)ethoxy]ethoxyl 2,3,4,6-tetra-*O*-acetyl-α-D-mannopyranoside (13). To a solution of **12** (0.61 g, 0.98 mmol, 1 equiv.) in DMF (30 mL) was added sodium azide (0.51 g, 7.84 mmol, 8 equiv.). The mixture was stirred at 80 °C 24 h. The reaction mixture was next diluted with ethyl acetate and the organic phase was washed with water and brine. The organic solvent was dried over Na_2SO_4 and concentrated under reduced pressure to afford **13** as colorless oil in 97% yield (0.47 g, 0.94 mmol). R_f = 0.35 (EtOAc/hexane, 1 : 4). ^{1}H NMR (300 MHz, $CDCl_3$): δ (ppm) 5.41–5.28 (m, 3H), 4.90 (d, J = 1.6 Hz, 1H), 4.32 (dd, J = 12.4, 5.1 Hz, 1H), 4.19–3.89 (m, 2H), 3.91–3.75 (m, 1H), 3.76–3.60 (m, 9H), 3.56–3.36 (t, J = 4.9 Hz, 2H), 2.16 (s, 3H), 2.11 (s, 3H), 2.06–2.03 (s, 3H), 2.00 (s, 3H); ^{13}C NMR (125 MHz, $CDCl_3$): δ (ppm) 170.7, 170.1, 170.0, 169.8, 97.8, 70.9, 70.8, 70.7, 69.6, 69.1, 68.4, 67.4, 62.5., 62.4, 50.7, 50.82, 21.0, 20.9, 20.8, 20.7. The spectroscopic data agreed with those of the literature.[38,39]

4.3.13 General procedure for synthesis of mannolipids (14–16)-method D. To a solution of 2-[2-(2-azidoethoxy)-ethoxy]ethoxyl 2,3,4,6-tetra-*O*-acetyl-α-D-mannopyranoside (**13**) (1.0 equiv.) and derivatives of bis (alkyloxy) benzoic acid, (**6–8**) (1.0 equiv.) in DCM (8.0 mL) was added tributylphopshine (1.5 equiv.) at 0 °C. The mixture was stirred at 0 °C for 2 h and then at the room temperature for 24 h. The presence of amine was confirmed by TLC. To reaction mixture hydroxybenzotriazole (HOBT) (1.6 equiv.) and *N*,*N*′-diisopropylcarbodiimide (DIC) (2.1 equiv.) were added and was stirred at room temperature for 96 h. The reaction was then diluted in ethyl acetate and the organic phase was washed with saturated $NaHCO_3$ solution and brine, dried and concentrated. The crude product was purified by column chromatography (hexane : EtOAc 1 : 0 to 7 : 3) to obtain compounds (**14–16**).

4.3.14 *N*-{*O*-[2-[(2-(2-(2,3,4,6-tetra-*O*-acetyl-α-D-mannopyranosyl)ethoxy)ethoxy)ethoxyl]]}-3,5-bis(dodecyloxy)benzamide (14). Compound (**14**) was prepared according to the general procedure **D** described above using (**13**) (100 mg, 0.2 mmol, 1 equiv.), **6** (98 mg, 0.20 mmol, 1 equiv.), tributylphosphine (60 μL, 0.324 mmol, 1.6 equiv.), HOBT (6.08 mg, 0.378 mmol, 1.9 equiv.) and DIC (42 μL, 0.328 mmol, 1.7 equiv.) in DCM (10 mL) in 77% yield (146 mg, 0.153 mmol). R_f = 0.35 (hexane-EtOAc 1 : 1). ^{1}H NMR (300 MHz, $CDCl_3$): δ (ppm) 6.86 (d, J = 2.2 Hz, 2H), 6.71 (t, J = 4.8 Hz, 1H), 6.52 (t, J = 2.1 Hz, 1H), 5.38–5.15 (m, 3H), 4.83 (d, J = 1.5 Hz, 1H), 4.25 (dd, J = 12.4, 5.1 Hz, 1H), 4.17–4.02 (m, 1H), 3.93 (t, J = 6.6 Hz, 4H), 3.84–3.75 (m, 2H), 3.68–3.56

(m, 11H), 2.14–1.93 (4s, 12H), 1.81–1.63 (m, 4H), 1.38–1.16 (m, 34H), 0.87 (t, J = 6.7 Hz, 6H); ^{13}C NMR (75 MHz, $CDCl_3$) δ (ppm) 170.6, 170.0, 169.9, 169.7 (4x CO), 167.4 (CO), 160.2 (C_{arom}), 136.6 (C_{arom}), 105.4 (CH_{arom}), 104.1 (CH_{arom}), 97.6 (C-1), 70.6, 70.3, 69.9, 69.8, 69.5, 69.0, 68.4, 68.2, 67.3, 66.1, 62.3, 39.8, 31.8, 29.6, 29.6, 29.5, 29.5, 29.3, 29.3, 25.9, 22.6, 14.0. ESI-HRMS: $[M + H]^+$ calcd for $C_{51}H_{85}NO_{15}$: 952.22, found 953.23.

4.3.15 *N*-{*O*-[2-[(2-(2-(2,3,4,6-tetra-*O*-acetyl-α-D-mannopyranosyl)ethoxy)ethoxy)ethoxyl]]}-3,5-bis(tetradecyloxy)benzamide (15). Compound **15** was prepared according to the general procedure **D** described above and isolated as colorless oil (174 mg, 0.172 mmol, 87%). R_f = 0.30 (hexane/ethyl acetate 1 : 1). ^{1}H NMR (300 MHz, $CDCl_3$) δ 6.90 (d, 2H, J H_{ortho}–H_{para} = 2.2 Hz, H_{ortho}), 6.71 (s, 1H, NH), 6.50 (s, 1H, H_{para}), 5.36 (dd, 1H, $J_{H2,H3}$ = 3.3 Hz, $J_{H3,H4}$ = 10 Hz, H3), 5.30 (dd, 1H, $J_{H3–H4}$ = 10 Hz, $J_{H4,H5}$ = 1.2 Hz, H4), 5.26 (dd, 1H, $J_{H1,H2}$ = 1.7 Hz, $J_{H2–H3}$ = 3.1 Hz, H2), 4.87 (d, 1H, $J_{H1–H2}$ = 1.7 Hz, H1), 4.28 (dd, 2H, $^3J_{H5–H6a}$ = 5.2 Hz, $J_{H6b–H6a}$ = 12.3 Hz, H6a), 4.09 (dd, 1H, $J_{H5–H6b}$ = 2.2 Hz, $J_{H6a–H6b}$ = 12.3 Hz, H6b), 4.06–4.02 (m, 1H, H5), 3.96 (t, 4H, J = 6.6 Hz, OCH_2), 3.85–3.76 (m, 1H, OCH_2), 3.72–3.60 (m, 11H, OCH_2), 2.18–1.76 (s, 12H, 4x CH_3), 1.90–1.57 (m, 6H, CH_2), 1.50–1.39 (m, 5H, CH_2), 1.38–1.19 (m, 42H, CH_2), 0.98–0.81 (m, 7H, CH_2); ^{13}C NMR (75 MHz, $CDCl_3$) δ (ppm) 169.6, 169.0, 168.9, 168.7 (4x CO), 166.4 (CO), 159.3 (C_{arom}), 135.6 (C_{arom}), 104.4 (CH_{arom}), 103.1 (CH_{arom}), 96.7 (C-1), 69.6, 69.3, 69.0, 68.5, 68.0, 67.4, 61.4, 38.8, 30.9, 28.6, 28.6, 28.6, 28.6, 28.5, 28.5, 28.3, 28.3, 24.9, 21.3, 19.7, 19.6, 13.0, 12.9, 12.5. ESI-HRMS: $[M + H]^+$ calcd for $C_{55}H_{94}NO_{15}$: 1008.6622, found 1008.6618.

4.3.16 *N*-{*O*-[2-[(2-(2-(2,3,4,6-tetra-*O*-acetyl-α-D-mannopyranosyl)ethoxy)ethoxy)ethoxyl]]}-3,5-bis(hexadecyloxy)benzamide (16). Compound **16** was prepared according to the general procedure **D** described above and isolated as colorless oil (167 mg, 0.156 mmol, 79%). R_f = 0.20 (hexane/ethyl acetate 1 : 1). ^{1}H NMR (300 MHz, $CDCl_3$) δ (ppm) 6.91 (d, 2H, $J_{ortho–para}$ = 2.2 Hz, H_{ortho}), 6.75 (s, 1H, NH), 6.57 (s, 1H, H_{para}), 5.38 (dd, 1H, $J_{H2,H3}$ = 3.3 Hz, $J_{H3,H4}$ = 10.5 Hz, H3), 5.32 (dd, 1H, $J_{H3–H4}$ = 10.5 Hz, $J_{H4,H5}$ = 1.2 Hz, H4), 5.28 (dd, 1H, $J_{H1,H2}$ = 1.7 Hz, $J_{H2–H3}$ = 3.3 Hz, H2), 4.88 (d, 1H, $J_{H1–H2}$ = 1.7 Hz, H1), 4.3 (dd, 2H, $J_{H5–H6a}$ = 5.2 Hz, $J_{H6a–H6b}$ = 12.4 Hz, H6a), 4.16–4.02 (m, 1H, H6b, H5), 3.97 (t, 4H, J = 6.5 Hz, OCH_2), 3.89–3.77 (m, 2H, OCH_2), 3.74–3.61 (m, 11H, OCH_2), 2.18–1.76 (s, 12H, 4x CH_3), 1.90–1.57 (m, 5H, CH_2), 1.52–1.10 (m, 50H, CH_2), 0.98–0.81 (m, 7H, CH_2); ^{13}C NMR (75 MHz, $CDCl_3$) δ (ppm) 170.7, 170.0, 169.9, 167.7 (4x CO), 167.5 (CO), 160.3 (C_{Ar}), 136.5 (C_{Ar}), 105.4 (CH_{Ar}), 104.2 (CH_{Ar}), 97.7 (C-1), 70.6, 69.5, 69.1, 68.4, 68.3, 66.1, 62.5, 42.3, 39.6, 31.9, 29.7, 29.6, 29.6, 29.4, 29.4, 29.3, 29.2, 28.3, 26.0, 23.3, 22.7, 20.8, 20.7, 20.7, 20.6, 14.12, 13.5. ESI-HRMS: $[M + H]^+$ calcd for C_{59} $H_{102}NO_{15}$: 1064.7244, found 1064.7210.

4.3.17 General procedure for de-*O*-acetylation of compounds (17–19)-method E. To a solution of (1 equiv.) of compounds (**14–16**) in dry MeOH (2 mL) was added NaOMe solution in 25 wt% in MeOH (0.5 equiv.) at room temperature under nitrogen atmosphere. After 3 h of stirring, the reaction mixture was neutralized with acidic resin Amberlite® IR120 H^+, filtered over a pad of Celite and concentrated *in vacuo* then then the solvent was removed *in vacuo*. The residue was then lyophilized to yield the fully deprotected final products (**17–19**).

4.3.18 *N*-{*O*-[(2-[2-(2-(α-D-Mannopyranosyl)ethoxy)ethoxy)-ethoxyl]]}-3,5-bis(dodecyloxy)benzamide (17). The crude residue (**14**) (60 mg, 0.063 mmol) was de-*O*-acetylated as above (NaOMe, MeOH, r.t., 4 h) (procedure **E**) to give (**17**) which was obtained in 98% yield (47.8 mg, 0.061 mmol) as a colorless oil. ^{1}H NMR (300 MHz, $CDCl_3$): δ (ppm) 7.07 (s, 1H), 6.91 (s, 2H), 6.55 (s, 1H), 5.11 (s, 2H), 4.85 (s, 1H), 3.94–3.87 (m, 8H), 3.76–3.62 (m, 14H), 2.94 (s, 2H), 1.74 (t, J = 6.9 Hz, 4H), 1.76–1.20 (m, 42H), 0.90 (t, J = 6.3 Hz, 6H); ^{13}C NMR (75 MHz, $CDCl_3$): δ (ppm) 167.7, 160.3, 136.3, 105.5, 104.3, 100.1, 72.3, 71.3, 70.9, 70.7, 70.2, 69.9, 68.4, 66.7, 66.4, 61.0, 40.0, 32.0, 29.8, 29.7, 29.6, 29.5, 29.4 29.3, 29.2, 26.1, 22.8, 14.2. ESI-HRMS: m/z calcd for $C_{43}H_{77}NO_{11}$: 783.5483; found $[M + H]^+$: 784.5557.

4.3.19 *N*-{*O*-[2-[(2-(2-(-α-D-Mannopyranosyl)ethoxy)ethoxy)-ethoxyl]]}-3,5-bis(tetradecyloxy)benzamide (18). The crude residue (**15**) was de-*O*-acetylated as above (NaOMe, MeOH, r.t., 4 h) to give (**18**) which was obtained in 97% yield (10.8 mg, 0.012 mmol) as a colorless oil. ^{1}H NMR (300 MHz, $CDCl_3$): δ (ppm) 7.07 (s, 1H), 6.91 (s, 2H), 6.55 (s, 1H), 5.11 (s, 2H), 4.85 (s, 1H), 3.94–3.87 (m, 8H), 3.76–3.62 (m, 14H), 2.94 (s, 2H), 1.74 (t, J = 6.9 Hz, 4H), 1.76–1.20 (m, 42H), 0.90 (t, J = 6.3 Hz, 6H); ^{13}C NMR (75 MHz, $CDCl_3$): δ (ppm) 167.3, 160.41, 136.3, 105.5, 104.3, 100.2, 72.3, 71.3, 70.9, 70.6, 70.1, 69.9, 68.3, 66.6, 66.3, 60.9, 39.9, 31.9, 29.7, 29.6, 29.5, 29.4, 29.3, 26.0, 22.7, 14.1. ESI-HRMS: m/z calcd for $C_{47}H_{85}NO_{11}$: 839.6123; found $[M + H]^+$: 840.6160.

4.3.20 *N*-{*O*-[2-[(2-(2-(-α-D-Mannopyranosyl)ethoxy)ethoxy)-ethoxyl]]}-3,5-bis(hexadecyloxy)benzamide (19). Compound (**16**) was de-*O*-acetylated as above (NaOMe, MeOH, r.t., 4 h) to give (**19**) which was obtained in 87% yield (25 mg, 0.028 mmol) as a colorless oil. ^{1}H NMR (600 MHz, $CDCl_3$): δ (ppm) 7.01 (s, 1H), 6.89 (s, 2H), 6.53 (s, 1H), 4.83 (s, 1H), 3.93 (s, 6H), 3.86 (s, 1H), 3.74 (s, 2H), 3.63 (d, J = 18.9 Hz, 10H), 1.74 (s, 4H), 1.65 (s, 2H), 1.42 (s, 5H), 1.41 (d, J = 6.9 Hz, 6H), 1.26 (s, 42H), 1.13 (s, 3H), 0.88 (s, 8H); ^{13}C NMR (150 MHz, $CDCl_3$): δ (ppm) 167.9, 160.3, 136.2, 105.5, 104.3, 100.0, 77.2, 77.0, 76.8, 70.8, 70.6, 70.2, 69.8, 68.3, 66.8, 66.6, 61.2, 42.4, 39.9, 31.9, 29.7, 29.6, 29.3, 29.2, 27.0, 26.6, 26.0, 24.1, 24.0, 23.4, 23.2, 22.7, 14.2; ESI-HRMS: m/z calcd for $C_{51}H_{93}NO_{11}$: 895.6754; found $[M + H]^+$: 896.6824.

4.4 Formulations and drug stocks

Stocks of **18** were prepared in *tert*-butanol (TBA) (Alfar Aesar, Ottawa ON) at 50 mg mL^{-1} and stored at 4 °C. A solution containing the DS derived from **18** was also prepared by combining the glycolipid with cholesterol (5 : 3 ratio w/w) in TBA. Nile Red (Sigma, St-Louis MO) stocks were prepared fresh in DMSO (Corning, Manassas VA) at 5 mg mL^{-1}. The liposomal formulations with Nile Red were prepared by combining 4 μL of 50 mg mL^{-1} **18** stock in TBA (final concentration 1 mg mL^{-1}) with 2 μL of 5 mg mL^{-1} Nile Red stock in DMSO (final concentration 100 μg mL^{-1}) and adding ddH_2O to a final volume of 100 μL (ratio 1 : 10 Nile Red : liposome). The formulations were further diluted in media as necessary for treatment. A stock solution of quercetin was generated in *tert*-butanol

(20 mg mL^{-1}), aliquoted and stored at −80 °C. The liposomal formulations with quercetin were prepared by combining the quercetin with the DS at a 1 : 5 w/w ratio. The preparation of quercetin/DS for HPLC analysis was prepared by combining 3 μL of the 20 mg mL^{-1} quercetin stock in TBA (final concentration 0.4 mg mL^{-1}) and 12 μL of the 25 mg mL^{-1} DS stock in TBA (final concentration 2 mg mL^{-1}) and adding either 135 μL of ddH_2O for entrapment studies, or 15 μL of ddH_2O and 120 μL of human plasma for plasma stability studies.

4.5 Cell culture

Blood from three healthy volunteers was collected in accordance to the Health Sciences North (HSN) Research Ethics Board protocol #18-061. PBMC were isolated by Ficoll-Paque (GE Healthcare, Uppsala, Sweden) density gradient immediately after blood collection, and were cryopreserved at 10^7 cells per mL in 90% heat-inactivated FBS (Gibco, Grand Island NY). Prior to experiments, cells were thawed, plated, and rested overnight before treatment. PBMC were maintained at 37 °C and 5% CO_2 in complete RPMI-1640 media (HyClone, Logan, UT, USA) supplemented with 10% heat-inactivated FBS and 100 units per mL streptomycin/penicillin (HyClone, Logan, UT, USA).

4.6 Cell viability

Toxicity in PBMC was measured using an apoptosis assay and lactate dehydrogenase (LDH) release. PBMC were seeded at 2×10^5 cells in 200 μL in 96-well plates. Cells were treated with 50 μg mL^{-1} of compound **18** for 48 hours. The collected cells were stained with Annexin V-FITC and propidium iodide (PI) (Invitrogen, Vienna, Austria) according to the manufacturer's protocol. Stained cells were analyzed using the Cytomics FC-500 flow cytometer (Beckman Coulter, Fullerton CA) and the CXP Analysis Software. LDH release was assessed in the supernatant of treated PBMC using the LDH-Cytox™ Assay Kit (Biolegend, San Diego CA) according to the manufacturer's protocol, with the absorbance measured at 490 nm. The % toxicity was calculated as followed:

$$\%\ \text{toxicity} = \frac{(\text{Abs test substance} - \text{Abs spontaneous})}{(\text{Abs max} - \text{Abs spontaneous})} \times 100$$

where test substance is the absorbance measured for **18**, spontaneous is the absorbance measured for untreated PBMC (0% toxicity), and max is the absorbance measure for lysed PBMC (100% toxicity). The media background absorbance was subtracted prior to calculating the cytotoxicity.

4.7 Cytokine analysis

PBMC were seeded at 10^6 cells per mL and left untreated or treated with 10 μg mL^{-1} of **18**. The cell supernatants were analyzed after 48 hours (for IL-6, IL-12p40 and IL-1β), or 7 days (for IFN-γ, IL-15 and IL-2). All kits were purchased from R&D Systems (Minneapolis, MN, USA) and ran according to the manufacturer's protocols.

4.8 Nile red uptake

Nile Red uptake was measured as previously described.[23] PBMC were treated with 10 μg mL^{-1} of empty **18**, 1 μg mL^{-1} of Nile Red, or 1 μg mL^{-1} of Nile Red entrapped in 10 μg mL^{-1} of **18**. Cells were incubated for 1 hour at 37 °C before collection. Adherent cells were collected using cell scrapers. The cells were washed once with 500 μL of PBS and resuspended in 500 μL of PBS for analysis. The mean fluorescence intensity (MFI) was analyzed using the Cytomics FC-500 flow cytometer using the FL3 channel where 3×10^4 events were measured. Data were analyzed using the CXP Analysis Software. The lymphocytes and monocytes were gated based on the forward and side scatter plot.

4.9 Human plasma collection

Blood was collected from healthy volunteers in EDTA blood collection tubes (BD Vacutainer, Mississauga Canada) in accordance to the Health Sciences North (HSN) Research Ethics Board protocol #18-061. Plasma was collected after centrifugation at 900 × *g* and 20 °C for 10 min with decreased deceleration, aliquoted, and stored at −80 °C.

4.10 HPLC conditions

All analyses were performed using a Shimadzu Prominence series HPLC system (Shimadzu Corporation, Kyoto, Japan), equipped with an LC-20AB binary pump (Serial: L20124200883), SIL-20A HT autosampler (Serial: L20345256104), CTO-20AC temperature-controlled column oven (Serial: L2021525077), SPD-M20A photodiode array detector and CBM-20A communications bus (Serial: L20235154327). All equipment were controlled by Shimadzu Lab Solutions Lite software version 5.71 SP2. For separation, an Ultra C18 column, 3 μm, 50 × 4.6 mm (RESTEK Corporation, Bellefonte, PA) was used. Quercetin samples were analyzed at a constant solvent flow rate of 1.0 mL min^{-1} at 35 °C using a binary gradient (Table A). Solvent A consisted of ddH_2O (0.2 μm filtered) and solvent B consisted of a 20% solution of acetonitrile (HPLC grade, Fisher Scientific, Fairlawn, NJ, USA) in ddH_2O, with each solvent containing 0.1% trifluoroacetic acid (v/v, protein sequencing grade, Sigma Aldrich, Fairlawn, NJ, USA).

4.11 Quercetin entrapment

The degree of entrapment for quercetin with the DS was assessed using a modified version of our previously reported methods.[20,21] Briefly, entrapment samples were setup in triplicate and stored overnight at 4 °C before analysis. The samples were gently vortexed for 5 minutes prior to centrifugation at 14 000 rpm for 10 minutes at room temperature. Supernatant were analyzed by RP-HPLC as above and the quercetin entrapment was calculated relative to the amount of quercetin in a control sample devoid of DS.

4.12 Plasma stability analysis

The stability of quercetin in human plasma, either alone or after glycoliposomal entrapment, was investigated according to previously published methods.[23] Samples were setup in

triplicate, with the mixtures gently vortexed for 5 min. Stability is represented as the percentage of compound remaining relative to the amount determined at T-zero.

4.13 Data analysis

All data was analyzed using Graph Pad Prism 5. Statistical analyses were performed using a two-way ANOVA with Bonferroni *post hoc* test, or an unpaired *t*-test.

Data availability

ESI,† includes NMR spectra of all compounds together with experimental details concerning CMC determination with tables and figures.

Conflicts of interest

The authors declare no conflict of interest.

Acknowledgements

This work was supported by a GlycoNet Collaborative Team grant (CR-25) awarded to Dr Roy & Dr Le. This work was also supported by a Discovery grant from the Natural Sciences and Engineering Research Council of Canada (NSERC, grant. No. RGPIN-2018-05570) awarded to Dr Roy. Further support was provided by the Northern Cancer Foundation (2023–2024) awarded to Dr Le.

References

1 S. Sapna Kumari, A. Goyal, E. S. Gürer, E. A. Yapar, M. Garg, M. Sood and R. K. Sindhu, Bioactive loaded novel nanoformulations for targeted drug delivery and their therapeutic potential, *Pharmaceutics*, 2022, **14**, 1091.
2 M. J. Mitchell, M. M. Billingsley, R. M. Haley, M. E. Wechsler, N. A. Peppas and R. Langer, Engineering precision nanoparticles for drug delivery, *Nat. Rev. Drug Discovery*, 2021, **20**, 101–124.
3 M. L. Etheridge, S. A. Campbell, A. G. Erdman, C. L. Haynes, S. M. Wolf and J. McCullough, The big picture on nanomedicine: the state of investigational and approved nanomedicine products, *Nanomedicine*, 2013, **9**, 1–14.
4 A. Z. Wilczewska, K. Niemirowicz, K. H. Markiewicz and H. Car, Nanoparticles as drug delivery systems, *Pharm. Rep.*, 2012, **64**, 1020–1037.
5 T. Keler, V. Ramakrishna and M. W. Fanger, Mannose-receptor-targeted vaccines, *Expert Opin. Biol. Ther.*, 2004, **4**, 1953–1962.
6 M. Paurević, M. Šrajer Gajdošik and R. Ribić, Mannose Ligands for Mannose Receptor Targeting, *Int. J. Mol. Sci.*, 2024, **25**, 1370.
7 J. M. Irache, H. H. Salman, C. Gamazo and S. Espuelas, Mannose-targeted systems for the delivery of therapeutics, *Expert Opin. Drug Delivery*, 2008, **5**, 703–724.
8 T. S. Patila and A. S. Deshpande, Mannosylated nanocarriers mediated site-specific drug delivery for the treatment of cancer and other infectious diseases: a state-of-the-art review, *J. Controlled Release*, 2020, **320**, 239–252.
9 A. Gupta and G. S. Gupta, Applications of mannose-binding lectins and mannan glycoconjugates in nanomedicine, *J. Nanopart. Res.*, 2022, **24**, 228.
10 F. Susa, S. Arpicco, C. F. Pirri and T. Limongi, An Overview on the Physiopathology of the Blood–Brain Barrier and the Lipid-Based Nanocarriers for Central Nervous System Delivery, *Pharmaceutics*, 2024, **16**, 849.
11 W. M. Pardridge, Drug transport across the blood-brain barrier, *J. Cereb. Blood Flow Metab.*, 2012, **32**, 1959–1972.
12 H. I. Chang and M. K. Yeh, Clinical development of liposome-based drugs: formulation, characterization, and therapeutic efficacy, *Int. J. Nanomed.*, 2012, **7**, 49–60.
13 B. S. Pattni, V. V. Chupin and V. P. Torchilin, New developments in liposomal drug delivery, *Chem. Rev.*, 2015, **115**, 10938–10966.
14 L. Sercombe, T. Veerati, F. Moheimani, S. Y. Wu, A. K. Sood and S. Hua, Advances and Challenges of Liposome Assisted Drug Delivery, *Front. Pharmacol.*, 2015, **6**, 286.
15 N. M. Al-Sawaftah, R. H. Abusamra and G. A. Husseini, Carbohydrate-functionalized liposomes in cancer therapy, *Curr. Cancer Ther. Rev.*, 2021, **17**, 4–20.
16 F. Chen, G. Huang and H. Huang, Sugar ligand-mediated drug delivery, *Future Med. Chem.*, 2020, **12**, 161–171.
17 H. Gao, C. Gonçalves, T. Gallego, M. François-Heude, V. Malard, V. Mateo, F. Lemoine, V. Cendret, F. Djedaini-Pilard, V. Moreau, C. Pichon and P. Midoux, Comparative binding and uptake of liposomes decorated with mannose oligosaccharides by cells expressing the mannose receptor or DC-SIGN, *Carbohydr. Res.*, 2020, **487**, 107877.
18 P. Valverde, J. D. Martínez, F. J. Cañada, A. Ardá and J. Jiménez-Barbero, Molecular Recognition in C-Type Lectins: The Cases of DCSIGN, Langerin, MGL, and L-Sectin, *ChemBioChem*, 2020, **21**, 2999–3025.
19 D. Goyard, T. C. Shiao, N. L. Fraleigh, H. Y. Vu, H. Lee, F. Diaz-Mitoma, H.-T. Le and R. Roy, Expedient synthesis of functional single-component glycoliposomes using thiol-yne chemistry, *J. Mater. Chem. B*, 2016, **4**, 4227–4233.
20 J. D. Lewicky, A. L. Martel, N. L. Fraleigh, A. Boraman, T. M. Nguyen, P. W. Schiller, T. C. Shiao, R. Roy and H.-T. Le, Strengthening peptide-based drug activity with novel glyconanoparticle, *PLoS One*, 2018, **3**, e0204472.
21 J. D. Lewicky, N. L. Fraleigh, A. Boraman, A. L. Martel, T. M. Nguyen, P. W. Schiller, T. C. Shiao, R. Roy, S. Montaut and H.-T. Le, Mannosylated glycoliposomes for the delivery of a peptide kappa opioid receptor antagonist to the brain, *Eur. J. Pharm. Biopharm.*, 2020, **154**, 290–296.
22 J. D. Lewicky, N. L. Fraleigh, A. L. Martel, T. M. Nguyen, P. W. Schiller, L. Mousavifar, R. Roy, A. D. Le, D. Funk and H.-T. Le, Improving the Utility of a Dynorphin Peptide Analogue Using Mannosylated Glycoliposomes, *Int. J. Mol. Sci.*, 2021, **22**, 7996.
23 L. Mousavifar, J. D. Lewicky, A. Taponard, R. Bagul, M. Rivat, S. Abdullayev, A. L. Martel, N. L. Fraleigh, A. Nakamura,

F. J. Veyrier, H.-T. Le and R. Roy, Synthesis & Evaluation of Novel Mannosylated Neoglycolipids for Liposomal Delivery System Applications, *Pharmaceutics*, 2022, **14**, 2300.

24 V. Percec, P. Leowanawat, H. J. Sun, O. Kulikov, C. D. Nusbaum, T. M. Tran, A. Bertin, D. A. Wilson, M. Peterca, S. Zhang, N. P. Kamat, K. Vargo, D. Moock, E. D. Johnston, D. A. Hammer, D. J. Pochan, Y. Chen, Y. M. Chabre, T. C. Shiao, M. Bergeron-Brlek, S. André, R. Roy, H.-J. Gabius and P. A. Heiney, Modular synthesis of amphiphilic Janus glycodendrimers and their self-assembly into glycodendrimersomes and other complex architectures with bioactivity to biomedically relevant lectins, *J. Am. Chem. Soc.*, 2013, **135**, 9055–9077.

25 S. Zhang, R. O. Moussodia, H. J. Sun, P. Leowanawat, A. Muncan, C. D. Nusbaum, K. M. Chelling, P. A. Heiney, M. L. Klein, S. André, R. Roy, H.-J. Gabius and V. Percec, Mimicking biological membranes with programmable glycan ligands self-assembled from amphiphilic Janus glycodendrimers, *Angew. Chem., Int. Ed.*, 2014, **53**, 10899–10903.

26 S. Zhang, R. O. Moussodia, C. Murzeau, H. J. Sun, M. L. Klein, S. Vértesy, S. André, R. Roy, H.-J. Gabius and V. Percec, Dissecting molecular aspects of cell interactions using glycodendrimersomes with programmable glycan presentation and engineered human lectins, *Angew. Chem., Int. Ed.*, 2015, **54**, 4036–4040.

27 Y. Azefu, H. Tamiaki, R. Sato and K. Toma, Facile synthesis of stable lipid analogues possessing a range of alkyl groups: application to artificial glycolipids, *Bioorg. Med. Chem.*, 2002, **10**, 4013–4022.

28 H. Tamiaki, Y. Azefu, R. Shibata, R. Sato and K. Toma, Oligomethylene spacer length dependent interaction of synthetic galactolipids incorporated in phospholipid layers with ricin, *Colloids Surf., B*, 2006, **53**, 87–93.

29 A. El Riz, A. Tchoumi Neree, L. Mousavifar, R. Roy, Y. Chorfi and M. A. Mateescu, Metallo-glycodendrimeric materials against enterotoxigenic *Escherichia coli*, *Microorganisms*, 2024, **12**, 966.

30 J. Li, S. Zacharek, X. Chen, J. Wang, W. Zhang, A. Janczuk and P. G. Wang, Bacteria Targeted by Human Natural Antibodies Using α-Gal Conjugated Receptor-Specific Glycopolymers, *Bioorg. Med. Chem.*, 1999, **7**, 1549–1558.

31 J. C. Medina-Rojas, I. O. Castillo-Rodríguez, E. Martínez-Klimova, T. Ramírez-Ápan, S. Hernández-Ortega and M. Martínez-García, Synthesis of flutamide-conjugates, *Biorg. Med. Chem. Lett.*, 2020, **30**, 127507.

32 A. Wagner, K. Vorauer-Uhl and H. Katinger, Liposomes produced in a pilot scale: production, purification and efficiency aspects, *Eur. J. Pharm. Biopharm.*, 2002, **54**, 213–219.

33 B. B. Agrawal and I. J. Goldstein, Physical and chemical characterization of concanavalin A, the hemagglutinin from jack bean (*Canavalia ensiformis*), *Biochim. Biophys. Acta*, 1967, **133**, 376–379.

34 R. D. Poretz and I. J. Goldstein, An examination of the topography of the saccharide binding sites of concanavalin A and of the forces involved in complexation, *Biochemistry*, 1970, **9**, 2890–2896.

35 D. Pagé and R. Roy, Synthesis and biological properties of mannosylated starburst poly(amidoamine) dendrimers, *Bioconjugate Chem.*, 1997, **8**, 714–723.

36 C. P. Swaminathan, N. Surolia and A. Surolia, Role of Water in the Specific Binding of Mannose and Mannooligosaccharides to Concanavalin A, *J. Am. Chem. Soc.*, 1998, **120**, 5153–5159.

37 C. W. Li, K. W. Hon, B. Ghosh, P. H. Li, H. Y. Lin, P. H. Chan, C. H. Lin, Y. C. Chen and K. K. Mong, Synthesis of oligomeric mannosides and their structure-binding relationship with concanavalin A, *Chem. – Asian J.*, 2014, **9**, 1786–1796.

38 A. V. Anand David, R. Arulmoli and S. Parasuraman, Overviews of biological importance of quercetin: A bioactive flavonoid, *Pharmacogn. Rev.*, 2016, **10**, 84–89.

39 R. Gugler, M. Leschik and H. J. Dengler, Disposition of quercetin in man after single oral and intravenous doses, *Eur. J. Clin. Pharm.*, 1975, **9**, 229–234.

40 S. V. Luca, I. Macovei, A. Bujor and A. Trifan, Bioactivity of dietary polyphenols: The role of metabolites, *Crit. Rev. Food Sci. Nutr.*, 2020, **60**, 626–659.

41 A. L. Martel, N. L. Fraleigh, E. Picard, J. D. Lewicky, G. Pawelec, H. Lee, G. W. Ma, L. Mousavifar, R. Roy and H.-T. Le, Novel immunomodulatory properties of low dose cytarabine entrapped in a mannosylated cationic liposome, *Int. J. Pharm.*, 2021, **606**, 120849.

42 J. D. Lewicky, A. L. Martel, N. L. Fraleigh, É. Picard, L. Mousavifar, A. Nakamura, F. J. Veyrier, F. Diaz-Mitoma, R. Roy and H.-T. Le, Exploiting the DNA Damaging Activity of Liposomal Low Dose Cytarabine for Cancer Immunotherapy, *Pharmaceutics*, 2022, **14**, 2710.

43 J. D. Lewicky, A. L. Martel, M. R. Gupta, R. Roy, G. M. Rodriguez, B. C. Vanderhyden and H.-T. Le, Conventional DNA-Damaging Cancer Therapies and Emerging cGAS-STING Activation: A Review and Perspectives Regarding Immunotherapeutic Potential, *Cancers*, 2023, **15**, 4127.